International Journal of Electrical and Computer Engineering (IJECE)
Vol. 12, No. 1, February 2022, pp. 157~165
ISSN: 2088-8708, DOI: 10.11591/ijece.v12i1.pp157-165

Optimal linear quadratic Gaussian control based frequency regulation with communication delays in power system

Hoan Bao Lai[1], Anh-Tuan Tran[1], Van Van Huynh[1], Emmanuel Nduka Amaefule[1], Phong Thanh Tran[1], Van-Duc Phan[2]
[1]Modeling Evolutionary Algorithms Simulation and Artificial Intelligence, Faculty of Electrical and Electronics Engineering, Ton Duc Thang University, Ho Chi Minh City, Vietnam
[2]Faculty of Automotive Engineering, School of Engineering and Technology, Van Lang University, Ho Chi Minh City, Vietnam

Article Info

Article history:

Received Sep 7, 2020
Revised Jun 23, 2021
Accepted Jul 2, 2021

Keywords:

Communication delay
Linear quadratic Gaussian
Load frequency control
Multi area power system

ABSTRACT

In this paper, load frequency regulator based on linear quadratic Gaussian (LQG) is designed for the multi-area power system (MAPS) with communication delays. The communication delay is considered to denote the small time delay in a local control area of a wide-area power system. The system is modeled in the state space with inclusion of the delay state matrix parameters. Since some state variables are difficult to measure in a real modern multi-area power system, Kalman filter is used to estimate the unmeasured variables. In addition, the controller with the optimal feedback gain reduces the frequency spikes to zero and keeps the system stable. Lyapunov function based on the linear matrix inequality (LMI) technique is used to re-assure the asymptotically stability and the convergence of the estimator error. The designed LQG is simulated in a two area connected power network with considerable time delay. The result from the simulations indicates that the controller performed with expectation in terms of damping the frequency fluctuations and area control errors. It also solved the limitation of other controllers which need to measure all the system state variables.

Corresponding Author:

Van Van Huynh
Modeling Evolutionary Algorithms Simulation and Artificial Intelligence, Faculty of Electrical and Electronics Engineering, Ton Duc Thang University
Ho Chi Minh City, Vietnam
Email: huynhvanvan@tdtu.edu.vn

1. INTRODUCTION

Automatic generation control (AGC) [i.e., automatic voltage regulator (AVR) and load frequency control (LFC)] for the multi-area power system (MAPS) has made the system highly economical and reliable to generate and transmit active power to load at safety frequency level and nearly nominal voltage in the modern MAPS under deregulated environment. From studies, the dependability of the active power to the load depends on the power regulation frequency. Therefore, frequency regulator is very important to keep frequency at the safe range in the MAPS. The job of frequency regulator otherwise known as the LFC is to retain the regulation frequency over randomly active power load changes sometimes known as disturbances. Another duty of the LFC is to control the tie-line power exchange error [1] that might exist in the MAPS. For simplicity, multi-area generating units are connected through tie-line communication link in other to ease the LFC. The use of this link introduces a new error called area control error (ACE) into the LFC. For example, if active power loads change affects one area, because the wide area power systems are interconnected through communication link. Therefore, this will not only affect the traditional governor speed control of the

generating area but also create control problems in the other areas. However, it is necessary for the area subjected to load change control and balance the fault within its area without other areas being affected. Otherwise, there is going to be an economic and reliability conflicts between different power generating companies tie together for example, GENCOS 1 and GENCOS 2 generating areas interconnected. Hypothetically, separated load frequency regulators are needed in each area to act swiftly during faults and able to set their setting parameters. Moreover, ACE signal receive by each controller is through the communication link, respectively. Therefore, the goal of control engineers is to develop the LFC to damping frequency error and ACE to the safe point after the disturbance has acted upon on any areas. The old proportional integral (PI), proportional integral derivative (PID) tuning based the LFC scheme [1] were applied to regulate frequency in the MAPS in the early days. However, with the complexity in modern power system, these controllers were seen degraded [1]. Recently, the development was made to use some algorithms combined with PID for the complex power system which were discussed in [2]-[9]. As power system becomes more complex, tuning parameters for the LFC becoming more complication. Therefore, the controller design needs to be robust enough to MAPS disturbances. Guo [10] the author applied sliding mode control (SMC) to control frequency in complex power system. However, SMCs were having chattering effect as a result of some neglected tuning parameters in the system model. The uses of SMC combined with some techniques to decrease chattering and minimize frequency error/ACE were discussed in [11]-[20]. Linear quadratic Gaussian technique was also designed and discussed in [21]-[25] for the complex wide area power system.

H-infinity scheme was also discussed in [26]-[27]. These controllers provided good performance and robust LFC in the wide area power system. Both SMC, linear quadratic Gaussian (LQG), H-infinity schemes worked well under power system with more tuning variables. However, the consideration of communication delay has brought a new era for the LFC of MAPS. These delays exist in power systems and vary from ten to several hundred on milliseconds. Communication links are used to connect ancillary components that are link connecting load frequency sensor point to the remote control unit (RCU) down to the generating unit. In reality, the RCU sometimes might experience delay in the receiving ACE signal. In practice, time-delay for the controller to receive input ACE signal should not be neglected and this signifies the optimal control. Therefore, communication delay should be taking into account in the dynamic modelling of complex power system. Newly published paper [28] addressed the LFC for the MAPS with time delay but with all system variables are assumed to be measured. In general, not all system parameters can be measured. The author work in [29] serves as a motivation to design a real conceptualization controller for the complex interconnected power plants with signal delay. In this paper, the LQR combined with Kalman filter technique are proposed as LQG method for frequency regulator of the MAPS with communication signal delay. The MAPS model is represented in state space with the time-delay to extend the model. This state space model is applied to obtain a better gain for the LQG. Since not all values of the LFC model's parameters are measurable. Therefore, Kalman filter is utilized for variables estimation. The estimations as well as time-delay are input signals. The contribution of the paper is stated below:

- Communication time delay is considered in the network state space model
- The proposed controller is designed based on state estimation with feedback gain and time delay
- Lyapunov theory and linear matrix inequality (LMI) techniques is used to prove the MAPS stability
- Comparison results are shown between the proposed controller and [29].

2. SYSTEM LFC MODEL IN TIME DELAY

In this section, a conceptualized LFC model taking into details with the time delay is discussed. A diagram describing two area power systems is display in Figure 1 [29]. Each area is represented with communication delay $e^{-s\tau}$. The value τ represents the small time delay which might varies from 0.1 to 1 s with consideration of two control areas for $i, j = 1,2 (i \neq j)$. Therefore, the modeled system with the information of the communication time delays is as (1).

$$\Delta \dot{P}_{tie,ij}(t) = 2\pi T_{ij}(\Delta f_i(t) - \Delta f_j(t)) \quad (1)$$

Other variables deviations are illustrated:

$$\Delta \dot{f}_i(t) = -\frac{1}{T_{pi}}\Delta f_i(t) + \frac{K_{Pi}}{T_{pi}}\Delta P_{mi}(t) - \frac{K_{Pi}}{T_{pi}}\Delta P_{tie,ij}(t) - \frac{K_{Pi}}{T_{pi}}\Delta P_{di} \quad (2)$$

$$\Delta \dot{P}_{mi}(t) = -\frac{1}{T_{ti}}\Delta P_{mi}(t) + \frac{1}{T_{ti}}\Delta P_{vi}(t) \quad (3)$$

$$\Delta\dot{P}_{vi}(t) = -\frac{1}{T_{gi}R_i}\Delta f_i(t) - \frac{1}{T_{gi}}\Delta P_{vi}(t) - \frac{1}{T_{gi}}\Delta E_i(t-\varepsilon_i) + \frac{1}{T_{gi}}u_i(t) \quad (4)$$

where $\Delta f_i(t)$ is the frequency deviation that is needed to be controlled, $\Delta P_{mi}(t)$ is the mechanical power change that requires generation-load balance during operation, ΔP_{di} is the disturbance affecting the system, $\Delta P_{tie,ij}(t)$ is the deviation in the net sum of the power exchange in the communication link connecting both area i and j. $\Delta E_i(t-\tau_i)$ which can be denoted as the ACE with communication delays and $u_i(t)$ is the control input to the system model.

$$\Delta\dot{E}_i(t) = K_{Bi}K_{ei}\Delta f_i(t) + K_{ei}\Delta P_{tie,ij}(t) \quad (5)$$

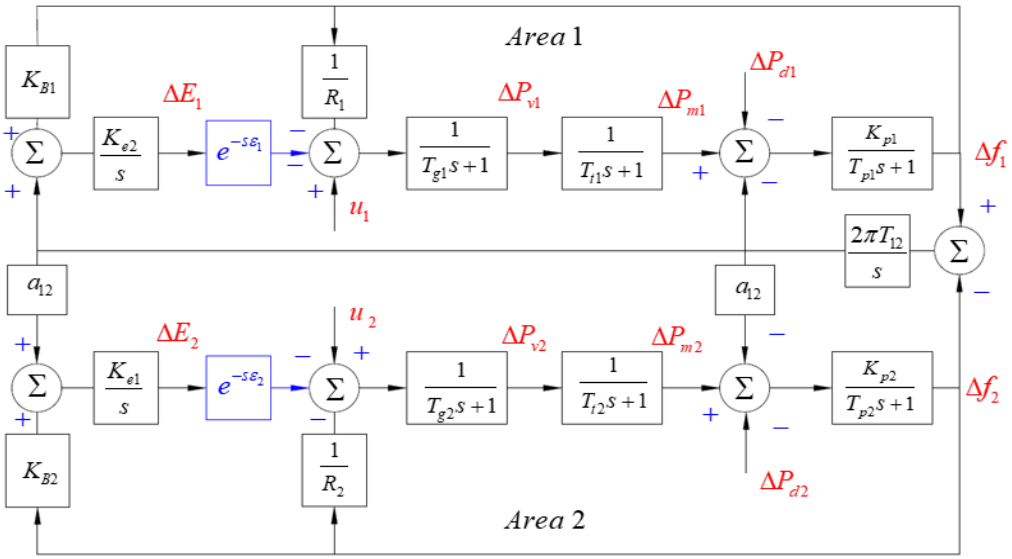

Figure 1. The structure of the two-area LFC model in a power system with time-delay

To represent the MAPS, the system state variables $\Delta f_i(t)$, $\Delta P_{mi}(t)$, $\Delta P_{vi}(t)$, $\Delta E_i(t)$, $\Delta P_{tie,ij}(t)$ are denoted as vector $x(t) = [\Delta A_{r1}\ \Delta P_{tie,12}\ \Delta A_{r2}]^T$ in which $\Delta A_{r1} = [\Delta f_1(t)\quad \Delta P_{m1}(t)\quad \Delta P_{v1}(t)\quad \Delta E_1(t)]$ and $\Delta A_{r2} = [\Delta f_2(t)\quad \Delta P_{m2}(t)\quad \Delta P_{v2}(t)\quad \Delta E_2(t)]$. The MAPS dynamic equations are derived above and it is suggested in the matrix form representation:

$$\dot{x}(t) = Ax(t) + A_{d1}x(t-\varepsilon_1) + A_{d2}x(t-\varepsilon_2) + Bu(t) + \Gamma\Omega(t)y(t) = Cx(t) \quad (6)$$

where $u(t) = [u_1\quad u_2]^T$ is the control signal vector and $\Omega(t) = [\Delta P_{d1}\quad \Delta P_{d2}]^T$ is the disturbance vector of the demands. For $l = 1,2$ and $b = 3,4$, the following matrices are defined as:

$$A = \begin{bmatrix} A_1 & A_3 & 0_{4\times4} \\ A_5 & 0_{1\times1} & -A_5 \\ 0_{4\times4} & a_{12}A_4 & A_2 \end{bmatrix};\ A_{dl} = \begin{bmatrix} 0 & 0 & -\frac{1}{T_{gl}} & 0 \end{bmatrix}^T;\ B = \begin{bmatrix} B_l & 0_{1\times5} \\ 0_{1\times5} & B_l \end{bmatrix}^T;\ \Gamma = \begin{bmatrix} \Gamma_l & 0_{1\times5} \\ 0_{1\times5} & \Gamma_l \end{bmatrix}^T$$

where $A_l = \begin{bmatrix} -\frac{1}{T_{pl}} & \frac{K_{p1}}{T_{p1}} & 0 & 0 \\ 0 & -\frac{1}{T_{tl}} & \frac{1}{T_{tl}} & 0 \\ -\frac{1}{R_lT_{gl}} & 0 & -\frac{1}{T_{gl}} & 0 \\ K_{Bl} & 0 & 0 & 0 \end{bmatrix};\ A_b = \begin{bmatrix} -\frac{K_{Pl}}{T_{pl}} & 0 & 0 & 1 \end{bmatrix}^T;\ A_5 = [2\pi T_{12} \quad 0 \quad 0 \quad 0]$

$$A_{td1} = \begin{bmatrix} 0_{4\times4} & A_{dl} & 0_{4\times5} \\ 0_{5\times4} & 0_{5\times1} & 0_{5\times5} \end{bmatrix};\ A_{td2} = \begin{bmatrix} 0_{5\times8} & 0_{5\times1} \\ 0_{4\times8} & A_{dl} \end{bmatrix};\ B_l = \begin{bmatrix} 0 & 0 & \frac{1}{T_{gl}} & 0 \end{bmatrix};\ \Gamma_l = \begin{bmatrix} -\frac{K_{Pl}}{T_{pl}} & 0 & 0 & 0 \end{bmatrix}$$

In the real system, exact measurement of the parameter values is impossible. Therefore, most parameters are approximated or estimated. Also, by considering time delay factor, so the dynamic model in (6) is further re-written as in (7):

$$\dot{x}(t) = [A + \Delta A(x,t)]x(t) + [A_{d1} + \Delta A_{d1}]x(t-\varepsilon_1) + [A_{d2} + \Delta A_{d2}]x(t-\varepsilon_2) + [B + \Delta B(x,t)]u(t) + \Gamma\Omega(t) = Ax(t) + A_{d1}x(t-\varepsilon_1) + A_{d2}x(t-\varepsilon_2) + Bu(t) + w(x,t)y(t) = Cx(t) + v(t) \quad (7)$$

where the unknown matrices $\Delta A(x,t)$ and $\Delta B(x,t)$ denote by system variations, the matrices A and B are the nominal values; $w(x,t)$ is called the total variations which can be estimated and we can define it in (8):

$$w(x,t) = \Delta A(x,t)x(t) + \Delta A_{d1}x(t-\varepsilon_1) + \Delta A_{d2}x(t-\varepsilon_2) + \Delta B(x,t)u(t) + \Gamma\Omega(t) \quad (8)$$

and $v(t)$ is a measurable disturbance. Ideally, some assumptions are stated to describe reality and the feasibility of the power system and as well the parameters based load frequency control strategies under certain conditions. These assumptions and some lemmas are stated below:

Assumption 1: If the matrix A, B is controllability, then, $\Delta A(x,t)$, $\Delta B(x,t)$ can be estimated.

Assumption 2: The lumped $w(x,t)$, which includes delay state matrix and the differential of $w(x,t)$ is bounded. i.e., there exist the known scalars γ and $\bar{\gamma}$ such that$\|w(x,t)\| \leq \gamma$ and$\|\dot{w}(x,t)\| \leq \bar{\gamma}$, where$\|.\|$ is matrix norm.

Lemma 1: [13] Let X, Y and F are actual matrices of appropriate dimension with $F^TF \leq 1$ then, for any scalar $\psi > 0$, the sequent matrix inequality holds.

$$XFY + Y^TF^TX^T \leq \psi^{-1}X^TX + \psi Y^TY$$

3. CONTROLLER DESIGN WITH TIME-DELAY

3.1. Linear quadratic regulator (LQR)

To design the LQG based LFC scheme for the described power system in Figure 1. The derived state space model is considered as shown in (7). In practice, the measurement of state variables is difficult and expensive because of lack of sensors. Therefore, the Kalman filter technique is realistic to estimate value of state variables. In addition, The Kalman filter can reject disturbances in form of white noise $v(t)$ which affect the system state. The greater problem is to get a better optimal gain K so that the eigenvalues $(A - BK)$ in (9) is places in their desired position and minimized a performance index below.

$$J = \frac{1}{2}\int [x^T(t)Q\,x(t) + u^T(t)Ru(t)]dt \quad (9)$$

Where $Q = E[w(x,t)]$ having dimension $(n \times n)$ and $R = E[v(x,t)]$ having dimension $(m \times m)$ both are a posited-definite Hermitian or real symmetric matrix. The LQG based controller can be designed in the time delay as in (10).

$$\dot{\hat{x}}(t) = A\hat{x}(t) + A_{d1}\hat{x}(t-\varepsilon_1) + A_{d2}\hat{x}(t-\varepsilon_2) + Bu(t) + K_e(y(t) - \hat{y}(t))\hat{y}(t) = C\hat{x}(t) \quad (10)$$

$\hat{x}(t)$ is the state variable estimation of the $x(t)$ of the observer and $y(t), \hat{y}(t)$ are output of the power network and observer, respectively. K_e is the gain, that is obtained from Riccati equation solution.

3.2. Proposed controller

The minimize *J* in (9) is designed with below controller:

$$u = -K\hat{x}(t) \quad (11)$$

where K is the optimal feedback gain for the LQR, $K = R^{-1}B^T\Re$ and $\Re$ is derived also from Riccati equation.

$$A^T\Re + \Re A - \Re BR^{-1}B^T\Re + Q = 0 \quad (12)$$

Substituting u into (6).

$$\dot{x}(t) = (A - BK)x(t) + BK\tilde{x}(t) + A_{d1}x(t - \varepsilon_1) + A_{d2}x(t - \varepsilon_2) + \Gamma\Omega(t) \quad (13)$$

Taking the error to be $\tilde{x}(t) = x(t) - \hat{x}(t)$ and $\dot{\tilde{x}}(t)$ is calculated as in (14):

$$\dot{\tilde{x}}(t) = \dot{x}(t) - \dot{\hat{x}}(t) = (A - K_eC)\tilde{x}(t) + A_{d1}\tilde{x}(t - \varepsilon_1) + A_{d2}\tilde{x}(t - \varepsilon_2) + \Gamma\Omega(t) \quad (14)$$

where $i = 1, 2$ are area number and from (1), (2) and (3), we obtained:

$$\begin{bmatrix}\dot{x}(t)\\ \dot{\tilde{x}}(t)\end{bmatrix} = \begin{bmatrix}(A - BK) & BK\\ 0 & (A - K_eC)\end{bmatrix}\begin{bmatrix}x(t)\\ \tilde{x}(t)\end{bmatrix} + \begin{bmatrix}A_{d1} & 0\\ 0 & A_{d1}\end{bmatrix}\begin{bmatrix}x(t - \varepsilon_1)\\ \tilde{x}(t - \varepsilon_1)\end{bmatrix} +$$

$$\begin{bmatrix}A_{d2} & 0\\ 0 & A_{d2}\end{bmatrix}\begin{bmatrix}x(t - \varepsilon_2)\\ \tilde{x}(t - \varepsilon_2)\end{bmatrix} + \begin{bmatrix}\Gamma\Omega(t)\\ \Gamma\Omega(t)\end{bmatrix} \quad (15)$$

Theorem 1: The system in (1) is asymptotic stable, if there exist matrices$R > 0, P > 0$ and positive scalars μ and γ such that the following LMIs hold:

$$\begin{bmatrix}(A - BK)^TR + R(A - BK) & RBK & RA_{d1} & RA_{d2} & R\Gamma & 0 & 0 & 0\\ K^TB^TR & (A - K_eC)^TP + P(A - K_eC) & 0 & 0 & 0 & PA_{d1} & PA_{d2} & R\Gamma\\ A^T{}_{d1}R & 0 & -\mu_1{}^{-1} & 0 & 0 & 0 & 0 & 0\\ A^T{}_{d2}R & 0 & 0 & -\mu_2{}^{-1} & 0 & 0 & 0 & 0\\ \Gamma^TR & 0 & 0 & 0 & -\mu_3{}^{-1} & 0 & 0 & 0\\ 0 & A^T{}_{d1}P & 0 & 0 & 0 & -\mu_1{}^{-1} & 0 & 0\\ 0 & A^T{}_{d2}P & 0 & 0 & 0 & 0 & -\mu_2{}^{-1} & 0\\ 0 & \Gamma^TR & 0 & 0 & 0 & 0 & 0 & -\mu_4{}^{-1}\end{bmatrix} < 0 \quad (16)$$

Proof: We choose Lyapunov function candidate as shadows

$$V(x(t), e(t)) = \begin{bmatrix}x(t)\\ \tilde{x}(t)\end{bmatrix}^T\begin{bmatrix}R & 0\\ 0 & P\end{bmatrix}\begin{bmatrix}x(t)\\ \tilde{x}(t)\end{bmatrix} + \int_{s_1}^{t}\begin{bmatrix}x(t - \varepsilon_1)\\ \tilde{x}(t - \varepsilon_1)\end{bmatrix}^T\begin{bmatrix}P_1 & 0\\ 0 & P_2\end{bmatrix}\begin{bmatrix}x(t - \varepsilon_1)\\ \tilde{x}(t - \varepsilon_1)\end{bmatrix}d(t - \varepsilon_1)$$
$$+ \int_{s_2}^{t}\begin{bmatrix}x(t - \varepsilon_2)\\ \tilde{x}(t - \varepsilon_2)\end{bmatrix}^T\begin{bmatrix}Q_1 & 0\\ 0 & Q_2\end{bmatrix}\begin{bmatrix}x(t - \varepsilon_2)\\ \tilde{x}(t - \varepsilon_2)\end{bmatrix}d(t - \varepsilon_2) \quad (17)$$

Then, the time derivative of $V(x(t), e(t))$ is indicated by (18).

$$\dot{V}(x(t), \tilde{x}(t)) = \begin{bmatrix}x(t)\\ \tilde{x}(t)\end{bmatrix}^T\begin{bmatrix}(A - BK)^TR + R(A - BK) & RBK\\ K^TB^TR & (A - K_eC)^TP + P(A - K_eC)\end{bmatrix}\begin{bmatrix}x(t)\\ \tilde{x}(t)\end{bmatrix}$$
$$+ \begin{bmatrix}x(t - \varepsilon_1)\\ \tilde{x}(t - \varepsilon_1)\end{bmatrix}^T\begin{bmatrix}A^T{}_{d1}R & 0\\ 0 & A^T{}_{d1}P\end{bmatrix}\begin{bmatrix}x(t)\\ \tilde{x}(t)\end{bmatrix} + \begin{bmatrix}x(t)\\ \tilde{x}(t)\end{bmatrix}^T\begin{bmatrix}RA_{d1} & 0\\ 0 & PA_{d1}\end{bmatrix}\begin{bmatrix}x(t - \varepsilon_1)\\ \tilde{x}(t - \varepsilon_1)\end{bmatrix}$$
$$+ \begin{bmatrix}x(t - \varepsilon_2)\\ \tilde{x}(t - \varepsilon_2)\end{bmatrix}^T\begin{bmatrix}A^T{}_{d2}R & 0\\ 0 & A^T{}_{d2}R\end{bmatrix}\begin{bmatrix}x(t)\\ \tilde{x}(t)\end{bmatrix} + \begin{bmatrix}x(t)\\ \tilde{x}(t)\end{bmatrix}^T\begin{bmatrix}RA_{d2} & 0\\ 0 & PA_{d2}\end{bmatrix}\begin{bmatrix}x(t - \varepsilon_2)\\ \tilde{x}(t - \varepsilon_2)\end{bmatrix}$$
$$+ \begin{bmatrix}x(t)\\ \tilde{x}(t)\end{bmatrix}^T\begin{bmatrix}P_1 & 0\\ 0 & P_2\end{bmatrix}\begin{bmatrix}x(t)\\ \tilde{x}(t)\end{bmatrix}d(t) - \begin{bmatrix}x(t - \varepsilon_1)\\ \tilde{x}(t - \varepsilon_1)\end{bmatrix}^T\begin{bmatrix}P_1 & 0\\ 0 & P_2\end{bmatrix}\begin{bmatrix}x(t - \varepsilon_1)\\ \tilde{x}(t - \varepsilon_1)\end{bmatrix}$$
$$+ \begin{bmatrix}x(t)\\ \tilde{x}(t)\end{bmatrix}^T\begin{bmatrix}Q_1 & 0\\ 0 & Q_2\end{bmatrix}\begin{bmatrix}x(t)\\ \tilde{x}(t)\end{bmatrix}d(t) - \begin{bmatrix}x(t - \varepsilon_2)\\ \tilde{x}(t - \varepsilon_2)\end{bmatrix}^T\begin{bmatrix}Q_1 & 0\\ 0 & Q_2\end{bmatrix}\begin{bmatrix}x(t - \varepsilon_2)\\ \tilde{x}(t - \varepsilon_2)\end{bmatrix}$$
$$+\Omega^T(t)\Gamma^TRx(t) + \Omega^T(t)\Gamma^TP\tilde{x}(t) + x^T(t)R\Gamma\Omega(t) + \tilde{x}^T(t)P\Gamma\Omega(t) \quad (18)$$

Applying Lemma 1 to (18),

$$\dot{V}(x(t), \tilde{x}(t)) \le \begin{bmatrix}x(t)\\ e(t)\end{bmatrix}^T\begin{bmatrix}\Theta_1 & RBK\\ K^TB^TR & \Theta_2\end{bmatrix}\begin{bmatrix}x(t)\\ e(t)\end{bmatrix} + \mu_5{\gamma_1}^2 + \mu_1{\gamma_2}^2 + \mu_2{\gamma_3}^2 \quad (19)$$

where
$\Theta_1 = (A - BK)^TR + R(A - BK) + \mu_1{}^{-1}RA_{d1}A^T{}_{d1}R + \mu_2{}^{-1}RA_{d2}A^T{}_{d2}R + \mu_3{}^{-1}R\Gamma\Gamma^TR$;
$\Theta_2 = (A - K_eC)^TP + P(A - K_eC) + \mu_1{}^{-1}PA_{d1}A^T{}_{d1}P + \mu_2{}^{-1}PA_{d2}A^T{}_{d2}P + \mu_4{}^{-1}R\Gamma\Gamma^TR$; $\mu_5 = \mu_3 + \mu_4$;
$\gamma_2 = \left\|\begin{bmatrix}x(t - \varepsilon_1)\\ \tilde{x}(t - \varepsilon_1)\end{bmatrix}\right\|$ and $\gamma_2 = \left\|\begin{bmatrix}x(t - \varepsilon_2)\\ \tilde{x}(t - \varepsilon_2)\end{bmatrix}\right\|$.

In addition, the LMIs (16) is equivalent to this inequality:

$$\begin{bmatrix} \Theta_1 & RBK \\ K^T B^T R & \Theta_2 \end{bmatrix} = -\Omega \tag{20}$$

and $-\Omega < 0$. Combining (16) and (19), we have:

$$\dot{V} \leq \sum_{i=1}^{N\Sigma} (-\lambda \|x(t)\|^2{}_{min} \tag{21}$$

where $\partial = \mu_5 {\gamma_1}^2 + \mu_1 {\gamma_2}^2 + \mu_2 {\gamma_3}^2$, the constant value ∂ and the eigenvalue λ_{min}. Hence, $\dot{V}<0$ is succeeded with $\|x(t)\| > \sqrt{\frac{\partial}{\lambda_{min}}}$. The system (15) is asymptotically stable.

4. RESULTS AND DISCUSSION

In this section, the MAPS with time delay are recommended to test the feasibility of the proposed LQG controller. The delays in the area control error signals of ε_1 and ε_2 are set to be fixed. The parameters of the area 1 and 2 generating unit are obtained from paper [29].

4.1. Simulation result based on nominal values

The parameters with their nominal values of the MAPS are used. All state variables are used in proposed controller is get from the Kalman filter. At this point, we assume step load disturbances occurring on the given system, $\Delta P_{d1} = 0.01$ pu at 0 s and $\Delta P_{d2} = 0.015$ pu at 0 s. The results of feedback signals are show in Figures 2, and 3 where Figure 2 is frequency deviation of area 1 and area 2, respectively. Figure 3 is tie-line power variation between two areas.

From these figures which show the time variation of the output signal, we can easily observed that frequency deviation in both areas converge to zero in 5 s with under shoot are -5×10^{-4} (pu MW) and -2.5×10^{-4} (pu MW) in the area 1 and area 2. From these results, it is obvious that proposed controller has good performance with soft settling times and small over/under shoots. These results of this controller are compared with other method in [29] in next case with the same conditions of disturbance and parameters of power system.

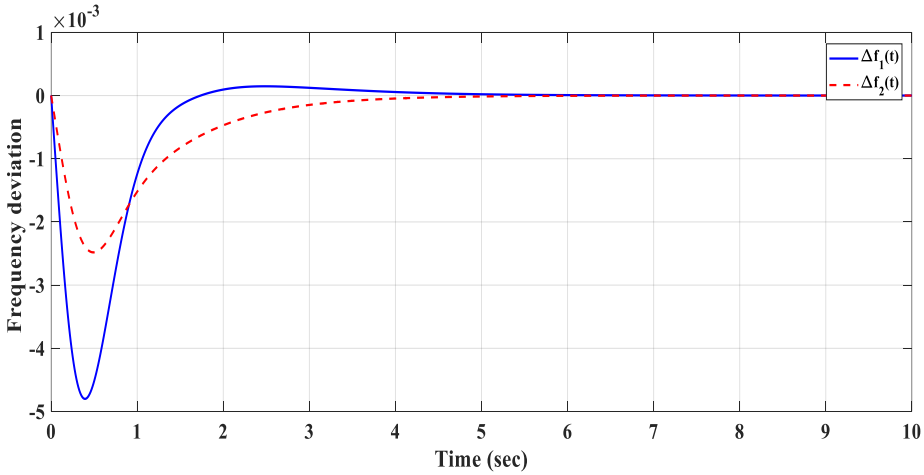

Figure 2. Frequency deviations (Hz) of the first-area and the second-area

4.2. Simulation result with random step change load disturbances

In Figures 4, the signals represent the random step change load turbulences for both area 1 and area 2. The random step load turbulences for the two areas network are generated in 200 s for this simulation. These load variations are applied to test proposed controller in difference conditions with reference to [29]. The simulation results for $\Delta f_1, \Delta f_2$ as in [29] are presented in Figure 5 and $\Delta P_{tie,12}$ at maximum tolerable delay margin in Figure 6, respectively. These results validates that the designed controller gain K is able to

achieve stabilization by minimizing the performance index better than [29] at same tolerable delay margin for random step load disturbances.

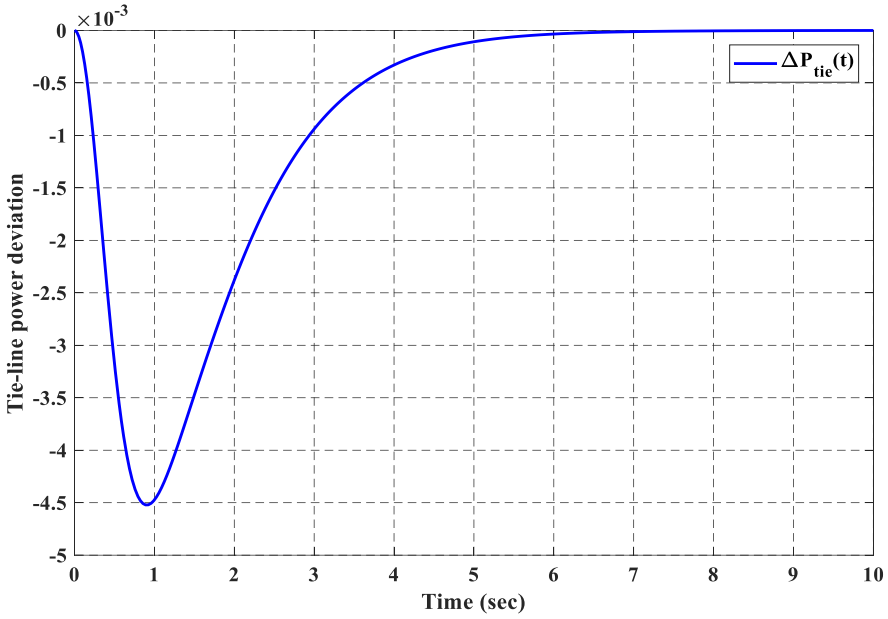

Figure 3. Tie line power deviation for power system

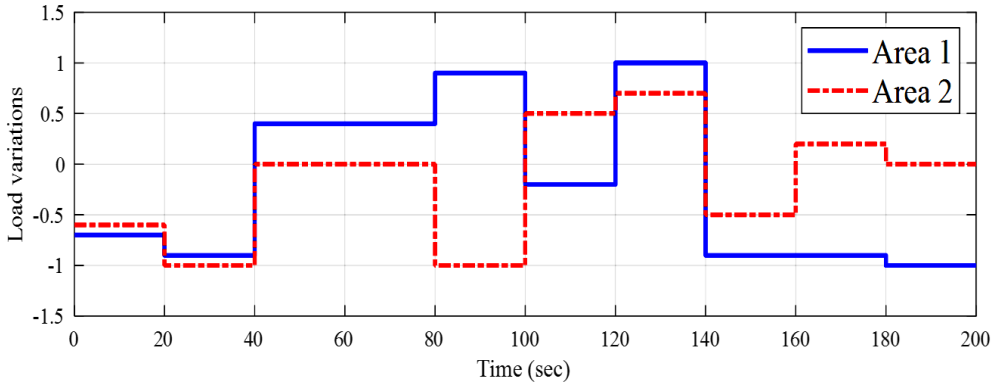

Figure 4. Load variations

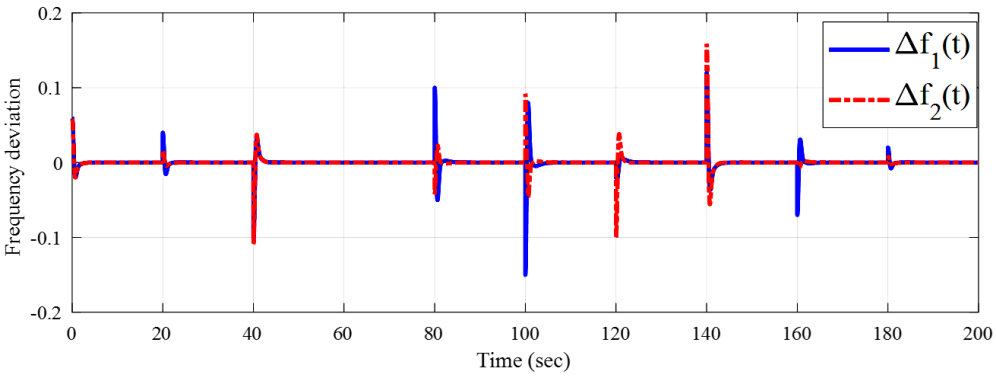

Figure 5. Frequency variations (Hz) of the two-area

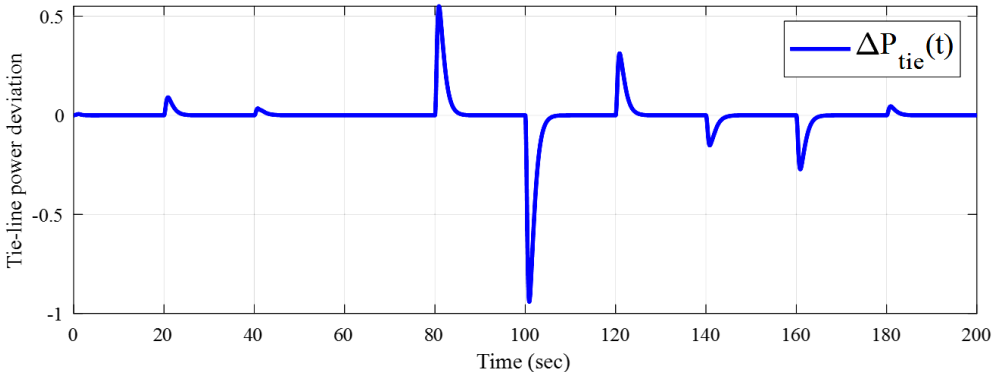

Figure 6. Tie-line variations

5. CONCLUSION

As expressed, the LFC based LQR is achieved for the wide area power network with communication delays. With regards to lack of sensors, the power system state variables are estimated by the Kalman filter. The optimal gain for the proposed controller is selected by solving the Riccati equation so that the control parameters are not over tuned. The stability of the system with time delay is again ascertained via Lyapunov theory. Results showed better performance to damp transient frequency and ACE than the controller compared with it. Also, some of the highlighted limitations from other controllers in literature are solved. However, the continuous difficulty in obtaining optimal control feedback gain using some schemes opens a new chapter to research area to develop and continuously improving the gain to avoid excessive tuning during linearization.

REFERENCES

[1] R. K. Sahu, S. Panda and N. K. Yegireddy, "A novel hybrid DEPS optimized fuzzy PI/PID controller for load frequency control of multi-area interconnected power systems," *Journal of Process Control*, vol. 24, no. 10, pp. 1596-1608, Oct. 2014, doi: 10.1016/j.jprocont.2014.08.006.

[2] S. Saxena and Y. V. Hote, "Decentralized PID load frequency control for perturbed multi-area power systems," *International Journal of Electrical Power and Energy Systems*, vol. 81, pp. 405-415, Feb. 2016, doi: 10.1016/j.ijepes.2016.02.041.

[3] T. K. Mohapatra and B. K. Sahu, "Design and implementation of SSA based fractional order PID controller for automatic generation control of a multi-area, multi-source interconnected power system," *Technologies for Smart-City Energy Security and Power*, pp. 1-6, Mar. 2018, doi: 10.1109/ICSESP.2018.8376697.

[4] N. E. Y. Kouba, M. Menaa, M. Hasni and M. Boudour, "Load frequency control in multi-area power system based on fuzzy logic-PID controller," *in International Conference on Smart Energy Grid Engineering (SEGE), 2015*, 2015, pp. 1-6, doi: 10.1109/SEGE.2015.7324614.

[5] A. G. Haroun and Y. Y. Li, "A novel optimized hybrid fuzzy logic intelligent PID controller for an interconnected multi-area power system with physical constraints and boiler dynamics," *ISA transactions*, vol. 71, pp. 364-379, Nov. 2017, doi: 10.1016/j.isatra.2017.09.003.

[6] A. Fathy, A. M. Kassem and A. Y. Abdelaziz, "Optimal design of fuzzy PID controller for deregulated LFC of multi-area power system via mine blast algorithm," *Neural Computing and Applications*, vol. 32, pp. 4531-4551, May 2020, doi: 10.1007/s00521-018-3720-x.

[7] K. Jagatheesan, B. Anand, S. Samanta, N. Dey, A. S. Ashour and V. E. Balas, "Design of a proportional-integral-derivative controller for an automatic generation control of multi-area power thermal systems using firefly algorithm," *IEEE/CAA Journal of Automatica Sinica*, vol. 6, no. 2, pp. 503-515, Jan. 2017, doi: 10.1109/JAS.2017.7510436.

[8] M. Raju, L. C. Saikia and N. Sinha, "Automatic generation control of a multi-area system using ant lion optimizer algorithm based PID plus second order derivative controller," *International Journal of Electrical Power and Energy Systems*, vol. 80, pp. 52-63, Sep. 2016, doi: 10.1016/j.ijepes.2016.01.037.

[9] Y. Arya and N. Kumar, "BFOA-scaled fractional order fuzzy PID controller applied to AGC of multi-area multi-source electric power generating systems," *Swarm and Evolutionary Computation*, vol. 32, pp. 202-218, Feb. 2017, doi: 10.1016/j.swevo.2016.08.002.

[10] J. Guo, "Application of full order sliding mode control based on different areas power system with load frequency control," *ISA transactions*, vol. 92, pp. 23-34, Sep. 2019, doi: 10.1016/j.isatra.2019.01.036.

[11] B. L. N. Minh, V. V. Huynh, T. M. Nguyen, and Y. W. Tsai, "Decentralized adaptive double integral sliding mode controller for multi-area power systems," *Mathematical Problems in Engineering*, vol. 1, pp. 1-11, Aug. 2018, doi: 10.1155/2018/2672436.

[12] K. Liao and Y. Xu, "A robust load frequency control scheme for power systems based on second-order sliding mode and extended disturbance observer," *IEEE Transactions on Industrial Informatics*, vol. 14, no. 7, pp. 3076-3086, Nov. 2017, doi: 10.1109/TII.2017.2771487.

[13] S. Prasad, S. Purwar and N. Kishor, "Load frequency regulation using observer based non-linear sliding mode control," *International Journal of Electrical Power and Energy Systems*, vol. 104, pp. 178-193, Jun. 2019, doi: 10.1016/j.ijepes.2018.06.035.

[14] V. V. Huynh, Y. W. Tsai, and P. V. Duc, "Adaptive output feedback sliding mode control for complex interconnected time-delay systems," *Mathematical Problems in Engineering*, pp. 1-15, 2015, doi: 10.1155/2015/239584.
[15] X. Lv, Y. Sun, Y. Wang, and V. Dinavahi, "Adaptive event-triggered load frequency control of multi-area power systems under networked environment via sliding mode control," *IEEE Access*, vol. 8, pp. 86585-86594, May 2020, doi: 10.1109/ACCESS.2020.2992663.
[16] Y. Mi, Y. Fu, C. Wang, and P. Wang, "Decentralized sliding mode load frequency control for multi-area power systems," *IEEE Transactions on Power Systems*, vol. 28, pp. 4301-4309, Nov. 2013, doi: 10.1109/TPWRS.2013.2277131.
[17] A. Dev and M. K. Sarkar, "Robust higher order observer based non-linear super twisting load frequency control for multi-area power systems via sliding mode," *International Journal of Control, Automation and Systems*, vol. 17, pp. 1814-1825, Jul. 2019, doi: 10.1007/s12555-018-0529-4.
[18] M. K. Sarkar, A. Dev, P. Asthana, and D. Narzary, "Chattering free robust adaptive integral higher order sliding mode control for load frequency problems in multi-area power systems," *IET Control Theory and Applications*, vol.12, pp. 1216-1227, May 2018.
[19] A. Dev, M. K. Sarkar, P. Asthan and D. Narzary, "Event-triggered adaptive integral higher-order sliding mode control for load frequency problems in multi-area power systems," *Iranian Journal of Science and Technology, Transactions of Electrical Engineering*, vol. 43, pp. 137-152, Jul. 2019, doi: 10.1007/s40998-018-0078-0.
[20] S. Trip, M. Cucuzzella, C. De Persis, A. Van der Schaft and A. Ferrara, "Passivity-based design of sliding modes for optimal load frequency control," *IEEE Transactions on control systems technology*, vol. 27, pp. 1893-1906, Jul. 2018, doi: 10.1109/TCST.2018.2841844.
[21] T. H. Mohamed, A. A. Z. Diab and M. M. Hussein, "Application of linear quadratic Gaussian and coefficient diagram techniques to distributed load frequency control of power systems," *Applied Sciences*, vol. 5, no. 4, pp. 1603-1615, Sep. 2015, doi: 10.3390/app5041603.
[22] M. Rahman, S. K. Sarkar and S. K. Das, "Stabilization improvement of load frequency deviation for multi-area interconnected smart grid using integral linear quadratic Gaussian control approach," *in 2018 10th International Conference on Electrical and Computer Engineering (ICECE)*, 2018, pp. 477-480, doi: 10.1109/ICECE.2018.8636686.
[23] M. Bhadu, N. Senroy, I. N. Kar and G. N. Sudha, "Robust linear quadratic Gaussian-Based discrete mode wide area power system damping controller," *IET Generation, Transmission and Distribution*, vol. 10, pp. 1470-1478, May 2016.
[24] S. H. Shahalami and D. Farsi, "Analysis of load frequency control in a restructured multi-area power system with the Kalman filter and the LQR controller," *AEU-International Journal of Electronics and Communications*, vol. 86, pp. 25-46, Mar. 2018, doi: 10.1016/j.aeue.2018.01.011.
[25] A. Al-Digs and Y. C. Chen, "Generation and load balance using linear quadratic Gaussian control," *North American Power Symposium*, vol. 3, pp. 1-5, Sep. 2016, doi: 10.1109/NAPS.2016.7747846.
[26] W. Yan, L. Sheng, D. Xu, W. Yang and Q. Liu, "H∞ robust load frequency control for multi-area interconnected power system with hybrid energy storage system," *Applied Sciences*, vol. 8, no. 10, 2018, Art. no. 1748, doi: 10.3390/app8101748.
[27] H. Zhang, J. Liu, and S. Xu, "H-infinity load frequency control of networked power systems via an event-triggered scheme," *IEEE Transactions on Industrial Electronics*, vol. 67, no. 8, pp. 7104-7113, Sep. 2019, doi: 10.1109/TIE.2019.2939994.
[28] S. Prasad, S. Purwar and N. Kishor, "H-infinity based non-linear sliding mode controller for frequency regulation in interconnected power systems with constant and time-varying delays," *IET Generation, Transmission and Distribution*, vol. 10, pp. 2771-2784, Aug. 2016.
[29] S. K. Pradhan and D. K. Das, "H∞ load frequency control design based on delay discretization approach for interconnected power systems with time delay," *Journal of Modern Power Systems and Clean Energy*, vol. 2, pp. 1-10, Aug. 2020, doi: 10.35833/MPCE.2019.000206.